

RSC Advances



This is an *Accepted Manuscript*, which has been through the Royal Society of Chemistry peer review process and has been accepted for publication.

Accepted Manuscripts are published online shortly after acceptance, before technical editing, formatting and proof reading. Using this free service, authors can make their results available to the community, in citable form, before we publish the edited article. This *Accepted Manuscript* will be replaced by the edited, formatted and paginated article as soon as this is available.

You can find more information about *Accepted Manuscripts* in the [Information for Authors](#).

Please note that technical editing may introduce minor changes to the text and/or graphics, which may alter content. The journal's standard [Terms & Conditions](#) and the [Ethical guidelines](#) still apply. In no event shall the Royal Society of Chemistry be held responsible for any errors or omissions in this *Accepted Manuscript* or any consequences arising from the use of any information it contains.

ARTICLE

pH responsive PVDF membrane with superwetting property for oil/water separation

Cite this: DOI: 10.1039/x0xx00000x

Received 00th January 2012,

Accepted 00th January 2012

DOI: 10.1039/x0xx00000x

www.rsc.org/

Yanhui Xiang, Jianhui Shen, Yunze Wang, Fu Liu* and Lixin Xue*

E-mail: fu.liu@nimte.ac.cn

E-mail: xuelx@nimte.ac.cn

Responsive materials with surfaces that have controllable oil wettability under water show out great potential for advanced applications. Here we report an economical and convenient methodology to fabricate superwetting PVDF membrane which obtains under oil superhydrophobicity and underwater superoleophobicity. This membrane is achieved by incorporating pH responsive N, N-dimethylaminoethyl methacrylate (DMAEMA) hydrogels into PVDF via a combination of in-situ polymerization and conventional phase separation technique. PDMAEMA chains can alter wettability as well as its conformation via protonation and deprotonation of its tertiary amine side groups in acidic water and pure water. Thus the membrane wettability underwater can be altered. Furthermore, we apply this responsive membrane for excellent separation of surfactant-stabilized water-in-oil and oil-in-water emulsions. High flux and separation efficiency together with excellent antifouling property are obtained and forebode our membranes have broad prospects in areas of oil/water separation.

Introduction

Stimulus-responsive polymers have attracted broad attention and been widely studied over the past decades due to their great potential in intelligent controlled materials.¹ Injection water in oil field, oil spill in sea, wastewater discharge in machining have long-term adverse impacts not only to the marine or land environment but also

to aquatic ecosystems.²⁻⁴ Eliminating oil spills in water remains currently a worldwide challenge, functional materials that can achieve oil/water separation efficiently gain enormous attraction.⁵⁻⁷ It is anticipated that a responsive surface that switches its wettability in response to external stimuli (light irradiation,^{8,9} electric fields,¹ temperature¹⁰ and pH^{11,12} etc) in aqueous media, would offer great

promise for advanced oil/water separation. Although considerable efforts have been contributed to controlling oil wettability as well as oil adhesion property on material surface under water, feasible method for producing responsive materials with switchable superoleophilicity (oil contact angle lower than 10°) and superoleophobicity (oil contact angle larger than 150°) surface underwater is still remaining to be further developed.

Felix Schacher's group fabricated a double stimuli-responsive membrane from polystyrene-block-poly(N, N-dimethylaminoethyl methacrylate) copolymers.¹³ Water flux, pore size and separation properties are able to respond to two independent stimuli (pH and temperature), but the further application was not studied probably due to the long term instability of the copolymer in harsh aqueous conditions. Recently, this stimuli-responsive material has been coated on a stainless steel mesh to realize oil/water separation.¹⁴

However, limited by stainless steel mesh substrates with pore size up to $40\ \mu\text{m}$, this mesh can only deal with free oil/water mixture and incapable of emulsion separation, especially in the presence of surfactant. A surface with switchable superoleophilicity and superoleophobicity in aqueous media was also realized on textiles and sponges by grafting pH responsive block copolymer poly(2-vinyl-pyridine) and polydimethylsiloxane (P2VP-b-PDMS).¹⁵ The modified material showed a selective permeation for water and oil due to the protonation and deprotonation of P2VP chains in responsive to the pH of aqueous media. Nevertheless, the material

preparation process is tough and time-consuming, besides, it is incapable of separating emulsified oil/water mixtures. In general, there are few reports on the feasible way to prepare superwetting PVDF membrane with responsive surfaces for surfactant-stabilized oil/water separation. In our previous work, we first reported an intelligent PVDF membrane which can separate both oil-in-water and water-in-oil emulsions.¹⁶ As most accepted, wettability is mainly governed by both surface chemistry and surface hierarchical structure.¹⁷⁻¹⁹ A hierarchical surface structure of PVDF membrane was created using a soft template stripping method to enhance its superwettability. As a consequence, the as-prepared membrane exhibits high permeability and excellent antifouling property. However, the expecting environmental responsive polymeric membrane is remained to be an interesting and challenging issue in practical application.

Herein, we present an economical and convenient methodology to fabricate a PVDF membrane with switch ability between underwater superoleophilicity to underwater superoleophobicity through pH responsive self-assembly. The prepared membrane showed excellent performances in treating both water-in-oil and oil-in-water emulsions. The membrane was prepared via a conventional non-solvent induced phase separation technique, and the pH responsive property was endowed to the membrane through an in-situ crosslinking method with N, N-dimethylaminoethyl methacrylate (DMAEMA) as a smart monomer and triethoxyvinylsilane (VTES)

as a crosslinker. The soft template stripping method was also applied to generate abundant surface microstructures.

Experimental

Materials

PVDF (FR904) was supplied by Shanghai 3F New Material Co., Ltd. China. DMAEMA, azodiisobutyronitrile (AIBN), n-hexane and bovine serum albumin (BSA, for molecular biology) were purchased from Shanghai Aladdin Chemistry Co., Ltd. China. After passing through an inhibitor-remover column (alkaline Al_2O_3), DMAEMA monomer was stored in a sealed clean vessel at 4 °C before use; initiator AIBN was recrystallized with n-hexane to remove inhibitors. VTES, hydrochloric acid, N, N-dimethylacetamide (DMAC), chloroform, dichloromethane and toluene were obtained from Sino pharm Chemical Reagent Co., Ltd. China. High purity of nitrogen was supplied by Wanli Gas of Ningbo, China. Unless specified, other chemical reagents were used as received.

Fabrication of pH responsive PVDF membrane

5.5 g DMAEMA, 1.0 g VTES, 0.08 g AIBN, together with 18 g PVDF and 130 g DMAC were added into a 250 mL three-necked bottle. The system oxygen was eliminated before heating up temperature by bubbling nitrogen through the solution for 30 min. After that, the polymerization was carried out at 80 °C with vigorous stirring and nitrogen atmosphere for 18 h. Next the homogenous casting solution was kept still overnight to remove any residual air bubbles and then cast uniformly onto PET non-woven fabric (NWF,

70 g/m^2) using a casting knife with a knife gap of 200 μm . The nascent membrane was immediately immersed into an inert non-solvent bath composed of DMAC/water mixture (v/v: 3/7) for 1 min, and then moved to pure water bath to complete total solidification. The PVDF membranes were dried in air after immersing in pure water for 48 h to eliminate solvent and possible unreacted monomers. The as-prepared sample was named as PVDF-PDMAEMA membrane.

Instruments and characterization

The morphology of as-prepared PVDF membrane and PET NWF were obtained with a field-emission scanning electron microscope (S-4800, Hitachi, Japan). The roughness of membrane surface was detected by an atomic force microscopy (AFM, Veeco Dimension 3100 V, US) in tapping mode with silicone tip cantilevers having a force constant of 20 mN/cm. The mechanical property of membrane was measured on a tensile tester (5567, Instron, US). The chemical compositions in the near bottom surface of the as-prepared membranes were analyzed by an X-ray photoelectron spectroscopy (XPS, Shimadzu Axis Ultradld spectroscopy, Japan) with Mg-K α as radiation resource. The take-off angle of the photoelectron was set at 90°. The functional groups on membrane bottom surface and the composition of emulsions were measured by attenuated total reflectance Fourier transform infrared spectra (ATR-FTIR, Thermo-Nicolet 6700, US). The content of PDMAEMA in membrane was evaluated by thermogravimetric analysis (TGA, Mettler-Toledo,

Switzerland) at 10 °C /min from 50 °C to 700 °C under a nitrogen flow (20 mL/min). Contact angles were measured by a contact angle meter (OCA20, Dataphysics, Germany), and at least five measurements were taken at different positions on each sample. UV-VIS spectra was determined using UV-VIS-NIR spectrometer (Lambda 950, Perkin Elmer, US). The purity of the purified filtrates was analyzed by Karl Fischer Titrator (Mettler Toledo DL, Switzerland). Optical microscopy images were taken on a BX 51TF Instec H601 (Olympus, Japan). The pH of water and BSA solution was determined with a pH meter (model 8685, China).

Preparation of water-in-oil and oil-in-water emulsions

For water-in-toluene (W/T), water-in-chloroform (W/C) and water-

in-dichloromethane (W/DCM) emulsion, span80 with a hydrophilic-lipophile balance (HLB) value of 4.3 was chosen as emulsifier, and pure water was applied; for toluene-in-water (T/W), chloroform-in-water (C/W) and dichloromethane-in-water (DCM/W) emulsion, tween80 with a HLB value of 15 was chosen as emulsifier, and acidic water with a pH of 2.0 (adjusted by hydrochloric acid) was applied. Practical preparation method and the droplet size of feed are shown in Table 1. The density and viscosity of the oils used in our work are listed in Table 2. All these mixtures were stirred for 3 h to obtain emulsions which were stable for more than 4 h and no demulsification or precipitation was observed.

Table 1. Practical preparation method and droplet size for oil/water emulsions.

Emulsion	Toluene (mL)	Chloroform (mL)	Dichloromethane (mL)	Span 80 (g)	Tween 80 (g)	Pure water (mL)	Acid water (mL)	Droplet size
W/T	80	--	--	0.135	--	2	--	500 nm ~10 μm
W/C	--	80	--	0.101	--	2	--	500 nm ~1 μm
W/DCM	--	--	80	0.070	--	0.8	--	500 nm ~1 μm
T/W	2	--	--	--	0.081	--	80	1 ~15 μm
C/W	--	2	--	--	0.050	--	80	100 nm ~1 μm
DCM/W	--	--	2	--	0.065	--	80	500 nm ~10 μm

Table 2. Density and viscosity of the oils used in this work.

Oil	Density (g/cm ³)	Viscosity (mPa S)
Toluene	0.866	0.587
Chloroform	1.498	0.563
Dichloromethane	1.327	0.430

Water flux through the membranes

The as-prepared pH responsive PVDF membrane was sealed between one vertical glass tube with an area of 3.14 cm² and one conical flask. A certain volume of water with different pH adjusted by hydrochloric acid was poured onto membrane. The flux measurement was carried out under an extra pressure (-0.09 MPa) generated by a vacuum driven filtration system, and was calculated from the permeation volume as a function of time. The water flux J (L/m² h) was defined as Equation (1):

$$J = \frac{V}{A\Delta t} \quad (1)$$

where V (L) was the volume of permeated water, A (m²) was the membrane area and Δt (h) was the permeation time.

Emulsion separation experiments

The apparatus and operating condition are identical as described in *Water flux through the membranes* section. After fixing the as-prepared membrane, an amount of freshly prepared emulsion was poured onto the PVDF membrane. The fluxes for emulsions were determined by Equation (1). For every emulsion, at least five samples were measured to obtain an average value and the finally obtained filtrate was collected for purity tests. To evaluate the stability separation of our membrane for oil/water emulsions, repeated emulsion separation experiments were carried out. After each experiment, the membrane was washed by ethanol to remove possible deposited surfactant and dried in oven at 40 °C.

Antifouling performance assessments

Due to the complicated oil/water separation condition, antifouling property is very important for membrane long-term use. The as-prepared PVDF membrane shows out different hydrophilicity (which is close related with membrane antifouling performance) whether PDMAEMA chains is protonation or deprotonation. Thus, the antifouling experiment was performed with acidic water (PDMAEMA chains is at protonation state) or pure water (PDMAEMA chains is at deprotonation state) and 1.0 g/L BSA solution prepared from corresponding water with the identical apparatus and operating condition described in *Water flux through the membranes* section. First, water was permeated through membrane, then BSA solution prepared from corresponding water was applied, the flux J_{w1} and J_{BSA} (L/m² h) for initial water and BSA solution respectively were calculated by Equation (1). After filtration of BSA solution, the membrane was rinsed with ethanol and water to recover the flux, then the water flux of cleaned membrane J_{w2} (L/m² h) was measured again by Equation (1). To analyze the antifouling property in details, several ratios were defined. The flux recovery ratio (FRR) was calculated by Equation (2):

$$FRR = \frac{J_{w2}}{J_{w1}} \times 100\% \quad (2)$$

a higher value of FRR implies a better antifouling property of membrane.

The reversible fouling ratio (DR_r) describes the flux decline caused by cake layer formation; the irreversible fouling ratio (DR_{ir}) indicates the non-recoverable flux decline induced by pore plugging and adsorption or deposition of foulants on membrane surface and pores; the total fouling ratio (DR_t) shows the total flux decline arises from the reversible fouling and irreversible fouling. These three ratios are expressed as follows:

$$DR_r = \frac{J_{w2} - J_{BSA}}{J_{w1}} \times 100\% \quad (3)$$

$$DR_{ir} = \frac{J_{w1} - J_{w2}}{J_{w1}} \times 100\% \quad (4)$$

$$DR_t = DR_r + DR_{ir} \quad (5)$$

Results and discussion

Morphology of pH responsive PVDF membrane

Generally, to achieve superwettability, a rough surface, especially a hierarchically micro-/nano-structured surface which amplifies the surface's intrinsic wetting behavior, is a prerequisite.^{1, 20-22} Here, a non-woven fabric was chosen as our soft template due to its low cost, easy availability and more importantly, its inherent concavo-convex rough surface, which provides membrane with unique micro/nano-structure besides micropores. Scanning electron microscopy measurement was carried out to explore the membrane surface peeled off from NWF and the inherent structure of NWF, as shown in Fig. 1a-c. A plenty of irregular grooves about 10 μm of width

endow membrane surface with great roughness. From the higher magnification image, circular micropores about 500 nm observed. The thickness of as-prepared membrane is around 65 μm . Finger-like pores are totally avoided and uniform cellular pores are generated, as shown in Fig. 1d-e. From the top surface of membrane (Fig. 1f), numerous litter white dots are produced by surface segregation of PDMAEMA-VTES during phase separation process. AFM measurement was applied to detect the roughness of membrane surface. The result in Fig. 2 indicates that the new surface peeled off from NWF gains an arithmetic mean surface roughness (Ra) of 940 nm, which is twice higher than the top surface (Ra = 419 nm) contacted with non-solvent directly. Furthermore, the as-prepared PVDF membrane exhibits a good mechanical strength with tensile strength of 5.3 MPa and elongation of 14.4 %, as shown in Fig. 3.

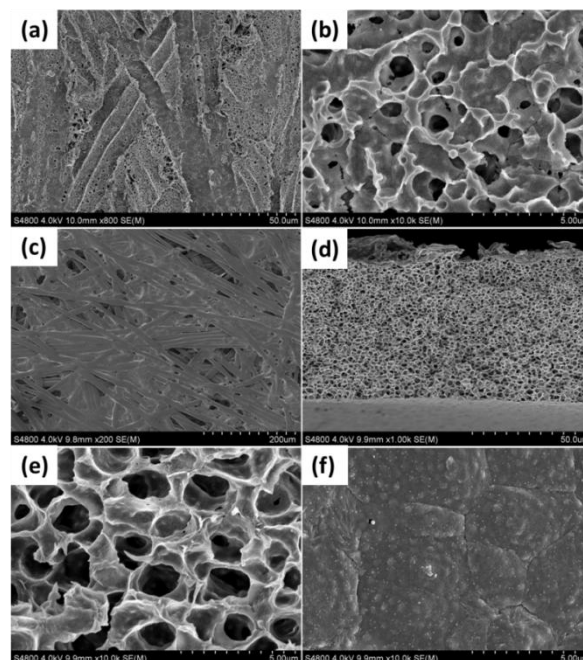


Fig. 1 Characterization for as-prepared PVDF membrane and NWF. (a,b) SEM images for PVDF membrane surface contacted with NWF; (c) SEM image for NWF surface; (d,e) SEM images for PVDF membrane cross section; (f) SEM images for PVDF membrane top surface.

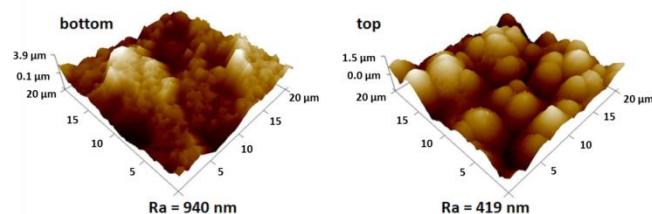


Fig. 2 3D AFM images for PVDF membrane surfaces (20 $\mu\text{m} \times 20 \mu\text{m}$).

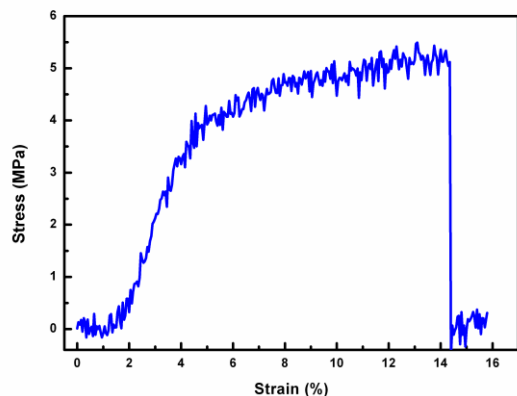


Fig. 3 Stress–displacement curve of the membrane (sized at 5 cm \times 1 cm)

Chemical composition of pH responsive PVDF membrane

To confirm the evidence that pH responsive PDMAEMA was indeed blended with PVDF membrane, pristine PVDF membrane was

fabricated as the control sample. The preparation method was similar with *Fabrication of pH responsive PVDF membrane* section, but without functional monomer DMAEMA, crosslinking VTES and initiator AIBN. XPS result was shown in Fig.4a, for pristine PVDF membrane, signals at 284, 686 eV ascribed to C, F elements are labeled; however for the as-prepared PVDF-PDMAEMA membrane, besides C, F elements, signals represent O, N and Si elements at 530, 396 and 154 eV respectively are presented as well, indicating that PDMAEMA together with crosslinker VTES is successfully blended and segregated to the membrane surface to some extents. According to the mass concentration of each element listed in Table 3, the content of the pH responsive PDMAEMA component in the membrane surface is calculated to be ~22 wt%. Characteristic peak around 1721 cm^{-1} attributed to C=O stretching vibration for ester group from FTIR-ATR spectra also implies existence of PDMAEMA, as shown in Fig.4b. TGA measurements were carried out to calculate the content of PDMAEMA in the membrane, and the result (Fig. 4c) shows that the membrane contains ~13 wt% pH responsive PDMAEMA. Compared to the XPS result, the difference value indicates a significant migration of PDMAEMA to membrane surface.

Table 3. Elements analysis of as-prepared PVDF membrane by XPS.

Elements	F	O	N	C	Si
----------	---	---	---	---	----

Atomic concentration (%)	36.06	6.75	2.64	53.02	1.54
Mass concentration (%)	45.36	7.15	2.44	42.17	2.87

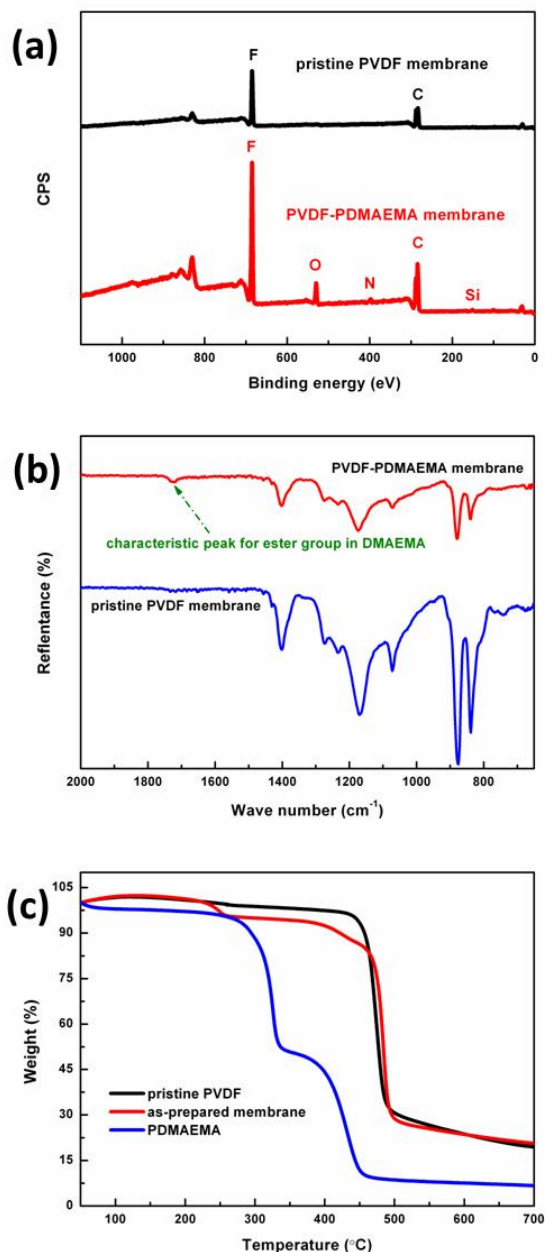


Fig. 4 (a) a wide-scan XPS spectra of pristine PVDF membrane and as-prepared PVDF-PDMAEMA membrane; (b) FTIR-ATR spectra for pristine PVDF membrane and as-prepared PVDF-PDMAEMA membrane; (c) TGA curves for newly synthesized PDMAEMA, pristine PVDF membrane and as-prepared PVDF-PDMAEMA membrane (PDMAEMA was synthesized by 5.5 g DMAEMA, 0.08 g AIBN at 80 °C with vigorous stirring and under nitrogen atmosphere for 18 h).

Wettability of pH responsive PVDF membrane

The tunable wettability was investigated by measuring the contact angle of PVDF membrane at aqueous media with different pH value, as shown in Fig. 5a. An acidic water droplet with a pH of 2.0 obtains a water contact angle (WCA) about $76 \pm 1^\circ$ in air, however the WCA for pure water droplet with a pH of 7.4 increases substantially up to $126 \pm 1^\circ$. The tunable wettability was closely related to the pH responsive PDMAEMA chains conformation via protonation and deprotonation of its tertiary amine side groups.^{23, 24} The pK_a of PDMAEMA is around 7.0. When the membrane surface contacts with an acidic water droplet with a pH of 2.0, the surface segregated PDMAEMA chains become protonated and exhibit an extended conformation due to the electrostatic repulsion among the like

charges, thus membrane surface acquires a relatively hydrophilic property. However, when the membrane is in contact with a water droplet with a pH of 7.4, PDMAEMA chains are deprotonated and exhibit a collapsed conformation due to hydrophobic interaction between deprotonated PDMAEMA chains. In this state, the water droplet mostly contacts with hydrophobic PVDF chains and leads to a larger WCA. PVDF membrane is naturally oleophilic due to the lower surface tension. As soon as oil (e.g. chloroform) droplet contacts the membrane surface, it immediately spreads out and the oil contact angle (OCA) decreases to $\sim 0^\circ$ within 1 s, indicating membrane superoleophilicity in air (Fig. 5b).

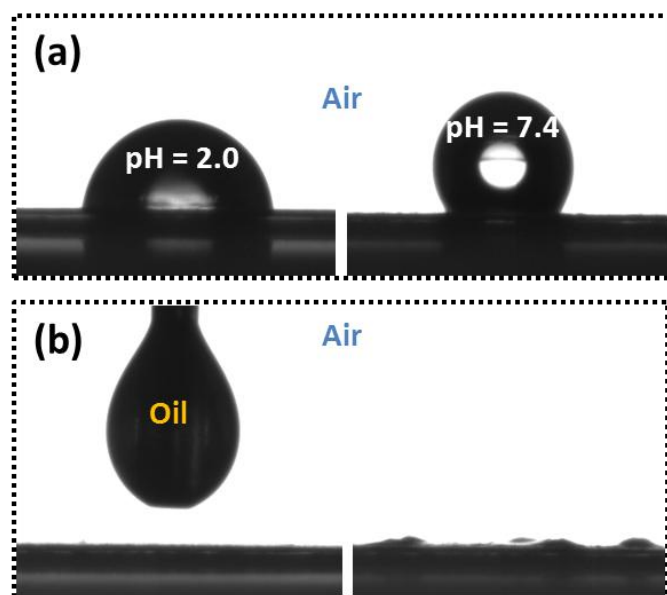


Fig. 5 Wettability and water flux with different pH of the as-prepared PVDF membrane. (a) static CA for water droplet (2 μL) with a pH of 2.0 and 7.4 applied on membrane bottom surface in air;

(b) static CA for oil droplet (chloroform, 3 μL) applied on membrane bottom surface in air.

In order to apply the pH responsive PVDF membrane in practical oil/water separation, under oil superhydrophobicity and underwater superoleophobicity are prerequisite. For this reason, both water wettability under oil and oil wettability underwater of membrane bottom surface (peeled from NWF) were evaluated. As shown in Fig. 6a, water droplets with a pH of 2.0 and 7.4 both attain quasi-spherical shape on membrane surface under oil with CA of $154 \pm 0.5^\circ$ and $153 \pm 0.7^\circ$ respectively, despite the pH value of water, indicating its under oil superhydrophobicity. In this state, the as-prepared membrane possessed the possibility for separating water-in-oil emulsions.

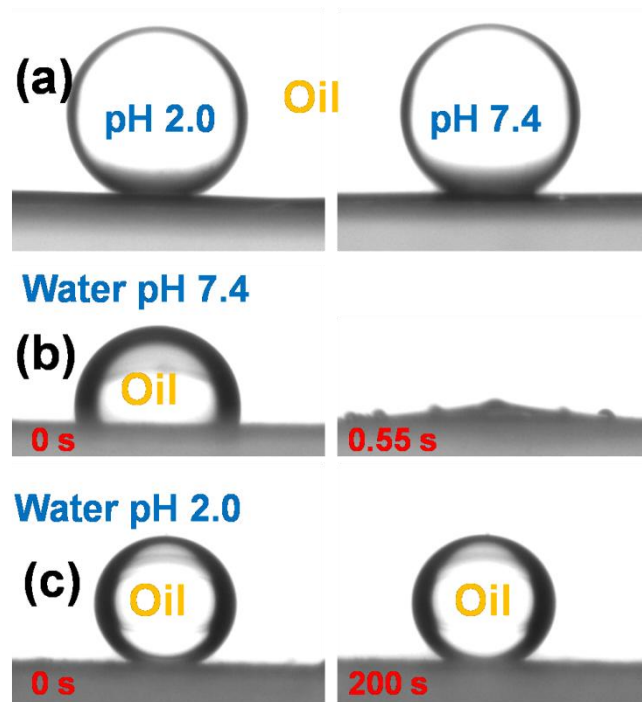
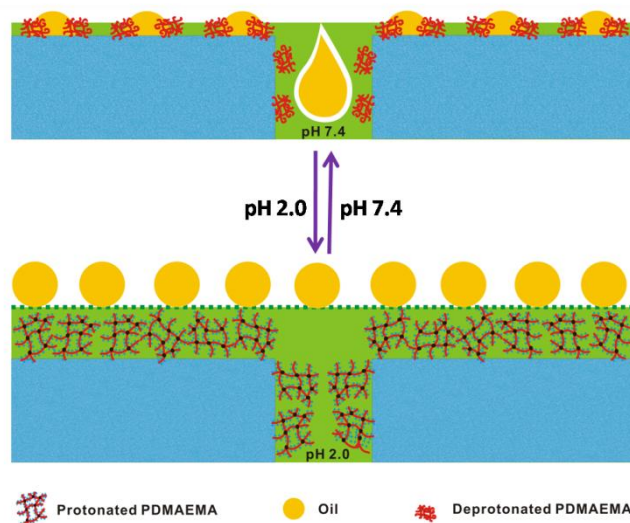


Fig. 6 Wettability of the as-prepared PVDF membrane in oil and water. (a) static CA for water droplet (4 μL) with a pH of 2.0 and 7.4 applied on membrane bottom surface in oil (n-hexane); (b) static CA for oil droplet (chloroform, 3 μL) applied on membrane bottom surface in pure water with a pH of 7.4; (c) static CA for oil droplet (chloroform, 3 μL) applied on membrane bottom surface in acidic water with a pH of 2.0 adjusted by hydrochloric acid.

To separate oil-in-water emulsion, the underwater superoleophobicity is a necessary feature for our membrane. However, when the membrane is immersed in pure water with pH 7.4, the instable water molecules layer is repelled from the deprotonated PDMAEMA network by oil (chloroform) droplet, which is immediately sucked into membrane within 0.55 s, implying underwater superoleophilicity, as shown in Fig. 6b. Thus in this state, the as-prepared membrane is incapable of separating oil-in-water emulsions. So as to overcome this boundedness, we took advantage of pH responsive property of PDMAEMA chains, adjusted the pH of aqueous media by hydrochloric acid to 2.0. When the pH responsive PVDF membrane is immersed in this acidic water, the oil droplet forms a sphere with a CA of $156 \pm 0.8^\circ$ and remained its initial shape within 200 s, seen in Fig. 6c. The mechanism of tunable affinity and pore size is proposed as shown in Scheme 1. When immersed in pure water (pH 7.4), deprotonated PDMAEMA network is dissatisfied of immobilization of water, and oil droplet almost passes through the

membrane with water, the obtained filtrate is just like the feed and demulsification can be neglected.; in constant, when contacted with acidic water (pH 2.0), PDMAEMA chains become protonated to generate a hydrophilic layer on membrane surface and the stable trapped water molecules layer blocks the access of oil (including initial small oil droplet and aggregated big oil droplet for demulsification),^{5, 25} displaying underwater superoleophobicity. As discussed previously, by adjusting the pH of aqueous media, the as-prepared pH responsive membrane gains the possibly for separating oil-in-water emulsions as well, amplifying the application in oil/water separation field.



Scheme 1 Schematic diagrams for the switchable oil wettability of PDMAEMA modified PVDF membrane under-water with a pH of 7.4 (up) or 2.0 (down).

Membrane wettability is considered to be controlled by cooperation between surface chemistry and microstructure, the influence of

former factor has been discussed particularly above, here we study the effect of hierarchical structure for amplification of under oil superhydrophobicity and underwater superoleophobicity by probing the wettability of membrane top surface (the surface contact non-solvent directly). The result shown in Fig.7 indicates that the WCA in oil of this smooth surface is only $139 \pm 1^\circ$ and OCA in acidic water (pH 2.0) is $120 \pm 3^\circ$. Compared with the rough surface peeled from NWF, this value is lower, and far from superwetting property. These results emphasize the importance of template stripping to enhance the microstructure of our membrane.

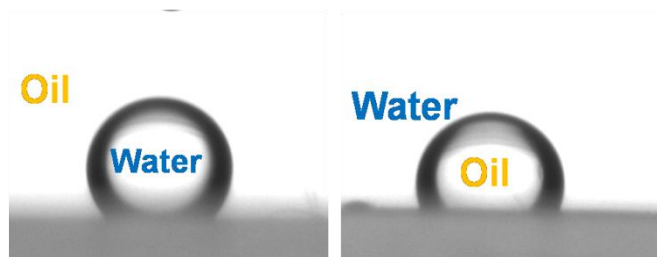


Fig. 7 Wettability for top surface of the as-prepared PVDF membrane in oil and water with a pH of 2.0. (a) static CA for a water droplet (2 μL) applied on membrane top surface in oil (n-hexane); (b) static CA for oil (chloroform) droplet (2 μL) applied on membrane top surface in water with a pH of 2.0.

Membrane flux inspired by water pH

Besides tunable wettability, the conformation variation of PDMAEMA will also alter the pore size of membrane responding to pH value variation. To testify this anticipation, water flux with

different pH was performed as shown in Fig. 8. In order to avoid the adverse influence of intrinsic instability of PVDF membrane in strong alkaline environment, only acidic and weak alkaline water were involved. The result demonstrates that the flux is around $16,000 \text{ L/m}^2 \text{ h}$ at pH 2.0 and increases enormously to $26,000 \text{ L/m}^2 \text{ h}$ at pH 6.5 and then decreases to $16,500 \text{ L/m}^2 \text{ h}$ at pH 7.5. The competitive balance between wettability and pore size determines the permeability variation. At low pH (2.0), PDMAEMA chains on membrane are highly protonated and stretched to diminish the pore size, thus lower water flux is obtained. However, when increasing pH below pK_a of PDMAEMA (7.0), PDMAEMA chains are partially protonated and shrunk to enlarge the pore size, thus the water flux is gradually increased. Nevertheless, at pH above pK_a , PDMAEMA chains are completely deprotonated and collapsed to expose more hydrophobic PVDF to membrane surface, therefore, the hydrophobicity property dominated the decreased water flux accordingly.

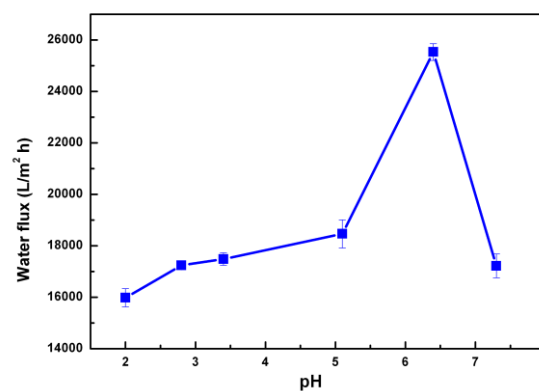


Fig.8 Membrane flux for water with different pH.

Separation performances of water-in-oil and oil-in-water emulsions

As mentioned above, our membrane possesses under oil superhydrophobicity and underwater superoleophobicity, which are prerequisites for separation of both water-in-oil and oil-in-water emulsions. To test separation capability of the as-prepared PVDF membrane, a series of surfactant-stabilized oil/water emulsions, namely water-in-toluene (W/T), water-in-chloroform (W/C), water-in-dichloromethane (W/DCM), toluene-in-water (T/W), chloroform-in-water (C/W) and dichloromethane-in-water (DCM/W) were prepared. For water-in-oil emulsions, oil is continuous phase which contacts membrane surface directly and water pH has nothing to do with separation effectiveness, as it has been proved that in oil, the membrane shows out superhydrophobicity with pure water, so this water was applied directly. Nevertheless, as discussed previously, this pH responsive membrane shows out superoleophilicity under pure water (pH 7.4) and superoleophobicity under acidic water (pH 2.0). With the purpose of separating oil-in-water emulsions, the pH of water for preparation of oil-in-water emulsions was adjusted to 2.0. The freshly prepared emulsions were poured onto membrane to carry out filtration separation under a vacuum pressure of 0.09 MPa. Fig. 9 gives a forthright result of effective separation of water-in-oil and oil-in-water emulsions (take water and toluene system as an

example) respectively by an optical microscope. Not a single droplet is observed in the collected filtrates. Compared to the original milky white feed emulsions, the collected filtrates are totally transparent, indicating the high rejection efficiency of the as-prepared membrane for separating both water-in-oil and oil-in-water emulsions.

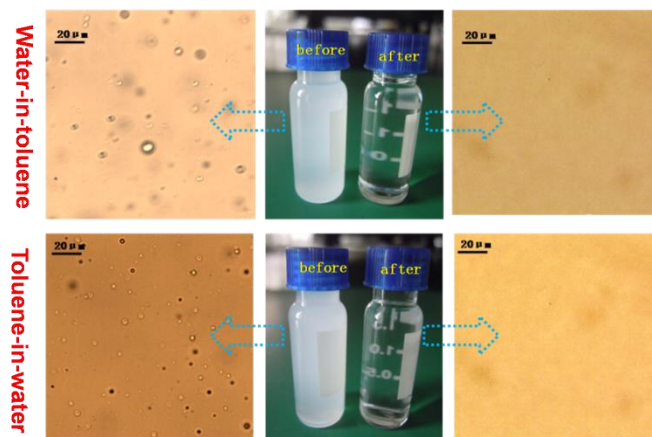


Fig. 9 Optical microscopy images for water-in-toluene emulsion (up) and toluene-in-water emulsion (down) before and after filtration.

Then UV-VIS and FTIR-ATR spectrometer were used to analyze the filtrates treated from oil-in-water emulsions. As shown in Fig. 10a, the absence of characteristic peak from UV-VIS spectrum for toluene confirmed the high rejection efficiency of our membrane. Similar effective separations are also achieved by FTIR-ATR experiment for other two emulsions, including C/W and DCM/W. The results shown in Fig. 10b and Fig. 10c indicated that characteristic peaks of chloroform and dichloromethane disappeared after separation process. The purity of all filtrates is listed in Table 4 and the value is above 99.9 %.

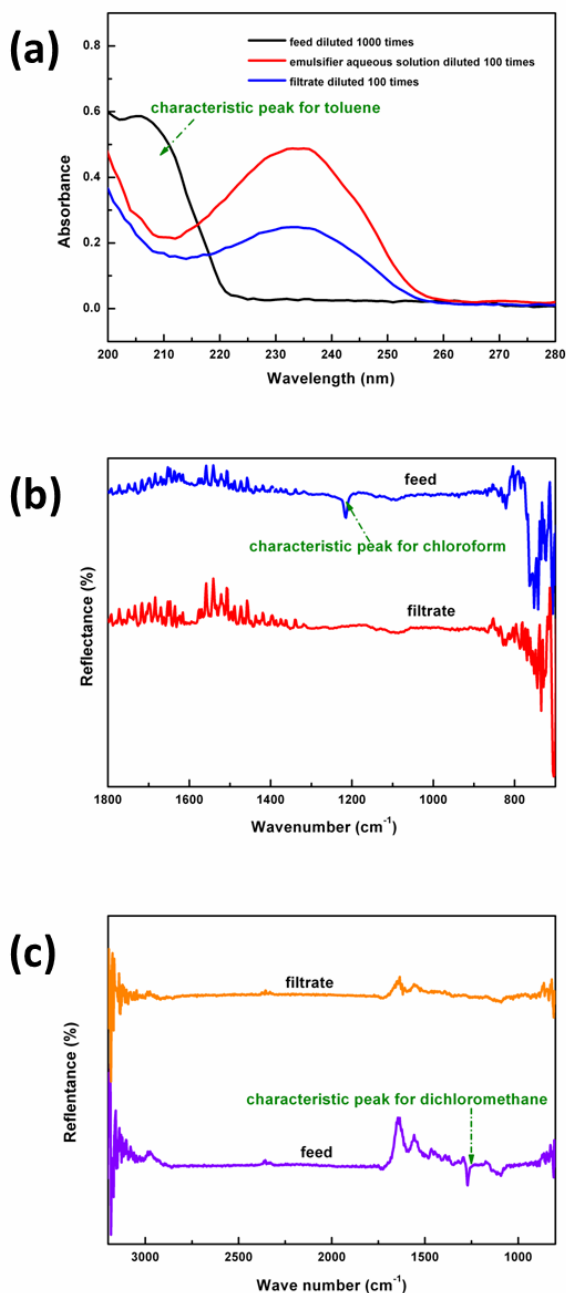


Fig.10 (a) UV-VIS spectra for toluene-in-water emulsion before and after filtration; (b) FTIR-ATR spectra for chloroform-in-water emulsion before and after filtration; (c) FTIR-ATR spectra for dichloromethane-in-water emulsion before and after filtration.

Table 4. Purity of filtrates for a variety of emulsions.

Emulsion	Purity of filtrate (%)
W/T	99.9928
W/C	99.9901
W/DCM	99.9964
T/W	99.9815
C/W	99.9912
DCM/W	99.9937

The flux of as-prepared membrane was measured including various water-in-oil and oil-in-water emulsions. As shown in Fig. 11, all emulsions exhibit high fluxes with 0.09 MPa of applied pressure across the membrane. The fluxes of 3347, 1680, 2798, 2574 L/m² h for span80 stabilized W/T, W/C and W/DCM and 1603, 1306, 1274 L/m² h for tween80 stabilized T/W, C/W and DCM/W respectively are obtained. These values are several times higher than those of traditional filtration membranes with similar permeation properties,^{26, 27} such separation performance is very attractive from the viewpoint of practical application.

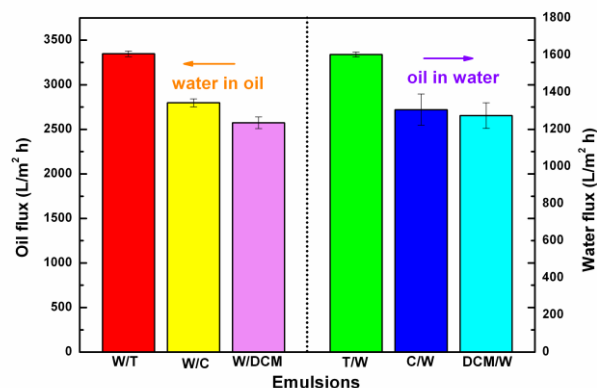


Fig. 11 The as-prepared membrane permeate flux for various emulsions.

Stability and antifouling properties of pH responsive PVDF membrane

In order to assess the stability oil/water separation of our membrane, ten times of repeated separation experiments were carried out, toluene and water system was taken as an example. As the results shown in Fig. 12a, during the experiments, both W/T and T/W keep stable flux value, around 3300 and 1600 L/m² h respectively. And the purity of filtrate from W/T and T/W is about 99.992% and 99.981% (Fig. 12b), indicating the good wettability, morphology and the mechanical strength were still preserved well. What's more, due to the complicated oil/water separation condition, unavoidable settlement and accumulation of foulants (including microorganisms, proteins and other organic molecules present in feed streams) on the membrane surface would hinder real applications of membrane technology.^{28, 29} In the first place, uncontrollable membrane fouling would lead to a decreased membrane performance, and thus enhanced operating pressure and chemical cleaning frequency need to maintain the initial membrane performance; besides, the frequent chemical cleaning may shorten the lifespan of membrane and increase maintenance cost of the membrane process.^{30, 31} Therefore, membrane antifouling property which is closely related with membrane hydrophilicity and low surface free energy is very

important for long-term practical use.^{27, 32-35} The repeated separation experiments do not take foulants such as protein into consideration. Here, to evaluate the antifouling property of our membrane, 1 g/L BSA solution prepared with pure water and acidic water was employed as a contaminant model. For each experiment, a certain volume of pure water, acidic water and BSA solution prepared with corresponding water permeated the membrane, and then the membrane was simply rinsed with ethanol and water to recover flux. The variation of flux during the process is revealed in Fig. 13a. It can be seen that when BSA solution was applied, the flux decreases to a relatively low value, however it recovers to a great extent after washing step. Further analysis of the membrane antifouling property in pure water and acidic water was also shown in Fig. 13b. The membrane flux recovery ratio (FRR) is 69 % and 97 % for pure water and acidic water respectively. The reversible fouling ratio (DR_r), irreversible fouling ratio (DR_{ir}) and total fouling ratio (DR_t) is 19 %, 31 % and 50 % for pure water, and 27 %, 3 % and 30 % for acidic water. Higher FRR value together with lower DR_t value indicates a better antifouling property in acidic water. Moreover, an increased DR_r and decreased DR_{ir} imply that in acidic water, protonated and stretched PDMAEMA chains make the membrane more hydrophilic, avoiding more BSA adsorption and deposition, and leading BSA to fall off from membrane surface by simple washing. These results indicate an excellent antifouling property of our membrane under acidic aqueous media.

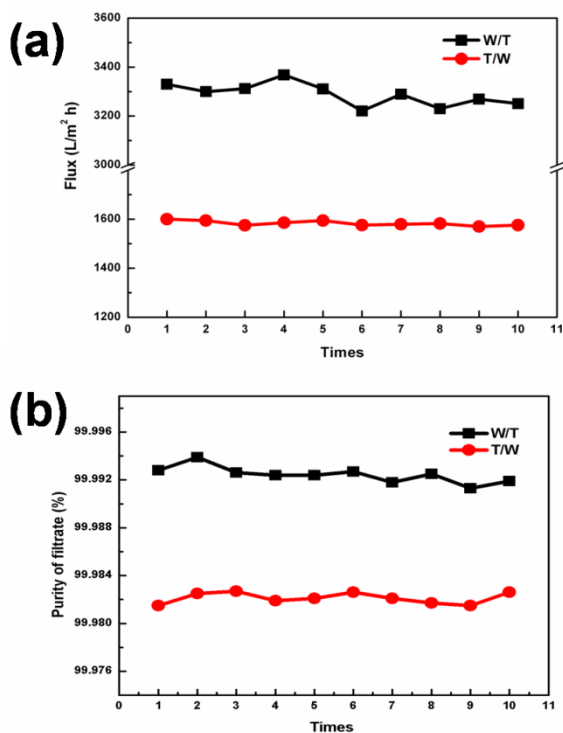


Fig.12 Results of water-in-toluene (W/T) and toluene -in-water (T/W) in ten times repeated separation experiments, after each separation process, the membrane was washed by ethanol and dried in oven at 40 °C. (a) flux of W/T and T/W in ten times repeated separation experiments; (b) purity of filtrate in ten times repeated separation experiments.

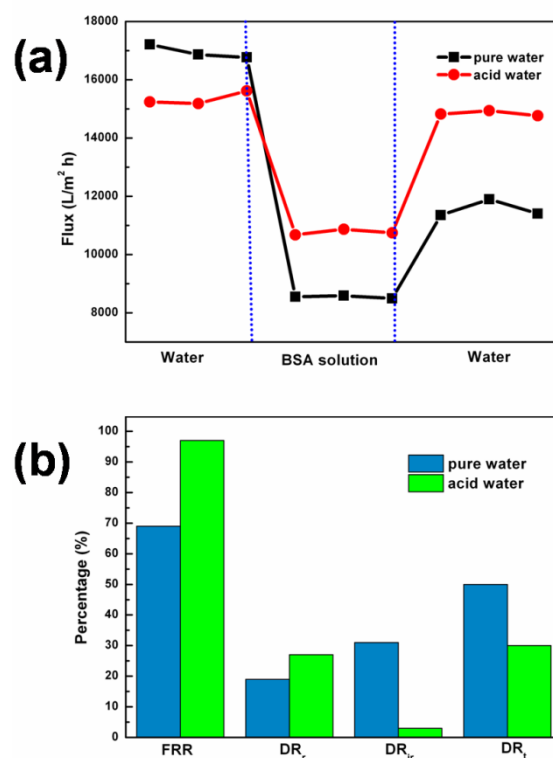


Fig. 13 Membrane antifouling property in pure water and acidic water with a pH of 2.0. (a) variation of flux and flux recovery by treating of water (pH 7.4 or 2.0) and BSA solution; (b) flux recovery ratio (FRR), reversible fouling ratio (DR_r), irreversible fouling ratio (DR_{ir}) and total fouling ratio (DR_t) for PVDF membrane in water with a pH of 7.4 or 2.0.

Conclusions

In summary, we have demonstrated that pH responsive membrane with under oil superhydrophobicity and underwater superoleophobicity can be achieved by incorporating DMAEMA hydrogels into PVDF via in-situ polymerization and phase separation, indicating its convenience and possibility to be produced

in a large scale. Under oil superhydrophobicity derived from hydrophobic PVDF chains, and has nothing to do with pH value of water. However, underwater wettability can be switched by pH value. In aqueous media with pH above pK_a , deprotonated and collapsed PDMAEMA chains lead to an underwater superoleophilic surface; nevertheless, in acidic water with pH below pK_a , the membrane surface with protonated and stretched PDMAEMA chains shows out underwater superoleophobicity. The responsive ability of the surface are attributed to the combined effect of the surface chemistry variation and rough structures. Furthermore, we apply this membrane for separation of surfactant-stabilized emulsions, including both water-in-oil and oil-in-water types. Relatively high flux and separation efficiency together with excellent antifouling property endow our membrane broad prospects for practical oil/water separation.

Acknowledgements

The authors appreciate financial supports from National Natural Science Foundation of China (No. 51273211, 51473177), the Ministry of Science and Technology of China (No. 2012AA03A605, 2012DFR50470), Bureau of Science and Technology of Ningbo (No. 2014B81004).

Notes and references

Polymer and Composite Division, Key Laboratory of Marine Materials and Related Technologies, Zhejiang Key Laboratory of Marine Materials and Protective Technologies
Ningbo Institute of Materials Technology & Engineering, Chinese Academy of Sciences, 1219 Zhongguan West Road, Ningbo 315201, China

- 1 B. Brugger and W. Richtering, *Adv. Mater.*, 2007, **19**, 2973-2978.
- 2 A. Jernelev, *Nature*, 2010, **466**, 182-183.
- 3 D. Dudgeon, A. H. Arthington, M. O. Gessner, Z. Kawabata, D. J. Knowler, C. Leveque, R. J. Naiman, A. H. Prieur-Richard, D. Soto, M. L. Stiassny and C. A. Sullivan, *Biol.Rev.Camb. Philos. Soc.*, 2006, **81**, 163-182.
- 4 C. Wu, C. Maurer, Y. Wang, S. Xue and D. L. Davis, *Environ. Health Perspect.*, 1999, **107**, 251-256.
- 5 Q. Wen, J. Di, L. Jiang, J. Yu and R. Xu, *Chem. Sci.*, 2013, **4**, 591-595.
- 6 L. Feng, Z. Y. Zhang, Z. H. Mai, Y. M. Ma, B. Q. Liu, L. Jiang and D. B. Zhu, *Angew. Chem. Int. Ed.*, 2004, **43**, 2012-2014.
- 7 Y. Zhu, F. Zhang, D. Wang, X. F. Pei, W. Zhang and J. Jin, *J. Mater. Chem. A*, 2013, **1**, 5758-5765.
- 8 M. Liu, F.-Q. Nie, Z. Wei, Y. Song and L. Jiang, *Langmuir*, 2010, **26**, 3993-3997.
- 9 X. Gui, Z. Zeng, Z. Lin, Q. Gan, R. Xiang, Y. Zhu, A. Cao and Z. Tang, *ACS Appl. Mater. Interfaces*, 2013, **5**, 5845-5850.
- 10 L. Chen, M. Liu, L. Lin, T. Zhang, J. Ma, Y. Song and L. Jiang, *Soft Matter*, 2010, **6**, 2708-2712.
- 11 A. K. Kota and A. Tuteja, *NPG Asia Mater.*, 2013, **5**, e58.
- 12 M. H. Tai, P. Gao, B. Y. L. Tan, D. D. Sun and J. O. Leckie, *ACS Appl. Mater. Interfaces*, 2014, **6**, 9393-9401.
- 13 F. Schacher, M. Ulbricht and A. H. E. Müller, *Adv. Funct. Mater.*, 2009, **19**, 1040-1045.
- 14 Y. Xiu, L. Zhu, D. W. Hess and C. Wong, *Nano lett.*, 2007, **7**, 3388-3393.
- 15 L. Zhang, Z. Zhang and P. Wang, *Npg Asia Materials*, 2012, **4**, e8.
- 16 M. Tao, L. Xue, F. Liu and L. Jiang, *Adv. Mater.*, 2014, **26**, 2943-2948.
- 17 H. Liu, S. Li, J. Zhai, H. Li, Q. Zheng, L. Jiang and D. Zhu, *Angew. Chem. Int. Ed.*, 2004, **43**, 1146-1149.
- 18 L. Feng, S. Li, H. Li, J. Zhai, Y. Song, L. Jiang and D. Zhu, *Angew. Chem.*, 2002, **114**, 1269-1271.
- 19 L. Feng, Y. Song, J. Zhai, B. Liu, J. Xu, L. Jiang and D. Zhu, *Angew. Chem.*, 2003, **115**, 824-826.
- 20 X. Huang, D. Kim, M. Im, J. Lee, J. Yoon and Y. Choi, *Small*, 2009, **5**, 90-94.

Journal Name

- 21 Y. Cao, X. Zhang, L. Tao, K. Li, Z. Xue, L. Feng and Y. Wei, *ACS Appl. Mater. Interfaces*, 2013, 130506143336000.
- 22 Y. Yang, Z. Tong, T. Ngai and C. Wang, *ACS Appl. Mater. Interfaces*, 2014, **6**, 6351-6360.
- 23 J. Karppi, S. Åkerman, K. Åkerman, A. Sundell, K. Nyysönen and I. Penttilä *Int. J. Pharm.*, 2007, **338**, 7-14.
- 24 X. Qiu, X. Ren and S. Hu, *Carbohydr. Polym.*, 2013, **92**, 1887-1895.
- 25 J. Chen, T. Liu, L. Zhao and W.-k. Yuan, *Ind. Eng. Chem. Res.*, 2013, **52**, 5100-5110.
- 26 B. Chakrabarty, A. K. Ghoshal and M. K. Purkait, *J. Membr. Sci.*, 2008, **325**, 427-437.
- 27 Z. Cheng, H. Lai, Y. Du, K. Fu, R. Hou, C. Li, N. Zhang and K. Sun, *ACS Appl. Mater. Interfaces*, 2014, **6**, 636-641.
- 28 D. Rana and T. Matsuura, *Chem. Rev.*, 2010, **110**, 2448-2471.
- 29 G. M. Geise, H. S. Lee, D. J. Miller, B. D. Freeman, J. E. McGrath and D. R. Paul, *J. Polym. Sci. Part B: Polym. Phys.*, 2010, **48**, 1685-1718.
- 30 V. Vatanpour, S. S. Madaeni, R. Moradian, S. Zinadini and B. Astinchap, *Sep. Purif. Technol.*, 2012, **90**, 69-82.
- 31 Y. Li, Y. Su, X. Zhao, X. He, R. Zhang, J. Zhao, X. Fan and Z. Jiang, *ACS Appl. Mater. Interfaces*, 2014, **6**, 5548-5557.
- 32 H. S. Sundaram, Y. Cho, M. D. Dimitriou, C. J. Weinman, J. A. Finlay, G. Cone, M. E. Callow, J. A. Callow, E. J. Kramer and C. K. Ober, *Biofouling*, 2011, **27**, 589-602.
- 33 J. A. Callow and M. E. Callow, *Nat. Commun.*, 2011, **2**, 244-254.
- 34 M. Zhang, C. Wang, S. Wang and J. Li, *Carbohydr. Polym.*, 2013, **97**, 59-64.
- 35 Y. Yang, H. Wang, J. Li, B. He, T. Wang and S. Liao, *Environ. Sci. Technol.*, 2012, **46**, 6815-6821.